EXPERIMENTAL RECREATION OF THE DIURNAL CYCLE AT THE PHOENIX LANDING SITE – INVESTIGATING THE FORMATION AND PERSISTENCE OF BRINE

E. Fischer, Department of Climate and Space Sciences and Engineering, University of Michigan, Ann Arbor, MI, USA *(erikfis@umich.edu)*, **G. M. Martínez**, Department of Climate and Space Sciences and Engineering, University of Michigan, Ann Arbor, MI, USA, **N. O. Renno**, Department of Climate and Space Sciences and Engineering, University of Michigan, Ann Arbor, MI, USA.

Introduction: The discovery of water ice in the shallow subsurface of polar and mid-latitude regions of Mars [1, 2, 3, 4, 5], as well as the discovery of perchlorate salts in the regolith of the polar and equatorial regions [6, 7, 8], suggests the possibility of temporary brine formation under present-day Martian conditions. Evidence for perchlorate salt hydration and brine formation has been suggested in regions from polar to equatorial latitudes on Mars [9, 10, 11, 12, 13].

We performed experiments to study the formation and persistence of brine throughout the polar Martian diurnal cycle at the Phoenix landing site. We use imaging and Raman scattering spectroscopy to detect liquid brine formation and disappearance. Here, we show results of experiments covering brine formation from perchlorate salt and water ice and investigate the persistence of brine throughout the polar diurnal cycle. We focus on calcium perchlorate because of this salt's presence at the Phoenix and Gale crater landing sites [6, 7], its suggested ubiquity on Mars [14], and its low eutectic temperature at 199 K [15].

Methods: We conducted our experiments in the Michigan Mars Environmental Chamber (MMEC). The MMEC is capable of simulating ground temperatures between 145 and 500 K, atmospheric pressures between 10 and 10^5 Pa, and a relative humidity (RH) from saturated conditions down to 5% RH at the lowest simulated temperatures and down to 1% at most Martian conditions [16].

The sample holder is a shallow cylindrical cavity of 10 mm in diameter, open to the chamber atmosphere. We use the visual images obtained by the camera as supporting evidence to the Raman spectra of the samples, because Raman spectra alone can be ambiguous when brine starts to form and the sample is heterogeneous, containing brine, crystalline salt and water ice. We use Gaussian decomposition on each obtained Raman spectrum throughout the entire diurnal cycles to search for changes in the phase of the samples. The wavenumber and Full Width Half Maximum (FWHM) of various spectral peaks are used to determine the phase of the samples by comparing them with reference values for crystalline perchlorate (salt), water ice, and liquid water [16].

In this abstract, we show the results of an experiment focusing on brine formation at the interface of separate water ice and salt layers and its persistence throughout an entire diurnal cycle. Martian examples for this are frost or snow deposition on the salt-containing regolith crust.

The environmental conditions simulated in the experiment correspond to sol 19 of the Phoenix mission. Sol 19 was chosen because, around this sol, soft white material suspected to be frozen brine [9, 10] was exposed by the robotic arm of the lander at a depth of ~5 cm [4], shown in Fig. 1. The environmental conditions of this sol were obtained from measurements and modeling, using a 1D hydrostatic column model developed to simulate environmental conditions at locations such as the Phoenix landing site (68°N) [17].

Fig. 2 shows the sol 19 environmental conditions and the conditions throughout the experiment in the MMEC. While the experimental ground temperature closely matches the sol 19 conditions, the frost point temperature in the experiment departs from the sol 19 diurnal cycle between 05:15 and 16:00 Local True Solar Time (LTST), suspected to be caused by previously trapped water on the chamber surfaces and by the sample itself, which is a source of additional water vapor throughout most of the experiment. We expect that this departure does not significantly affect the results of our experiment.

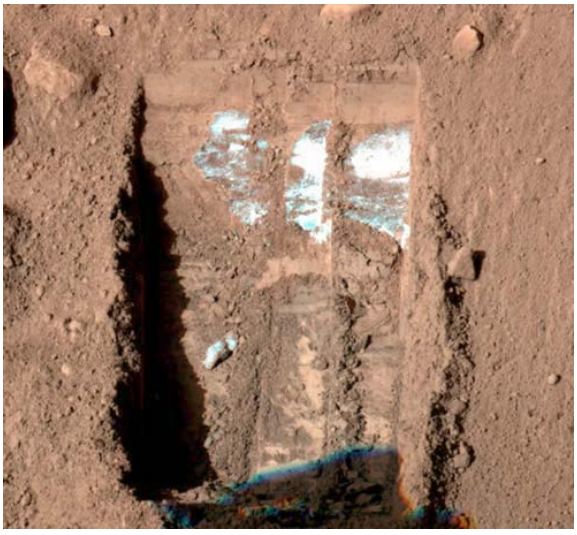

Figure 1. *Image of the trench dug by Phoenix, exposing the soft, white material on sol 19 [9].*

Results: Fig. 3 shows the changes in the O-H vibrational band of the Raman spectrum throughout the

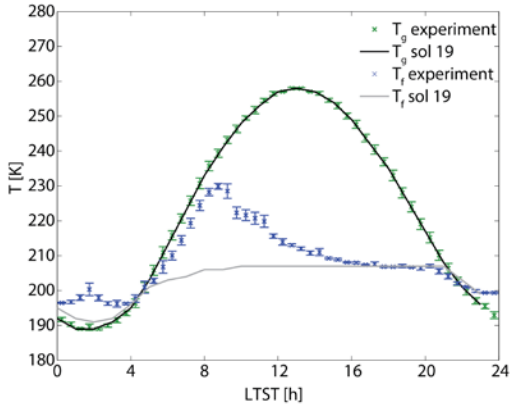

Figure 2. *Environmental conditions on sol 19 of the Phoenix mission and simulated in our environmental chamber. The black and gray lines represent values from numerical simulations of the ground temperature and frost point of the surrounding air at the Phoenix landing site, while green and blue crosses represent the temperature and frost point measured inside the MMEC.*

diurnal cycle on the ground and Fig. 4 shows the corresponding (color-coded) visual images of the sample. Table 1 shows the peaks obtained by Gaussian decomposition of the curves in Fig. 3.

The narrow spectral peaks at 00:10 LTST in Fig. 3 and Table 1, shortly after the beginning of the diurnal cycle are indicative of a hydrated crystalline perchlorate salt, in this case calcium perchlorate. Correspondingly, the image in Fig. 4a shows a crystalline salt on top of the ice layer. The first visual evidence for brine formation can be seen at 05:15 in Fig. 4b, shortly after crossing the eutectic temperature in the diurnal cycle (Fig. 2). The Raman spectrum (Fig. 3, blue line) and its decomposition in the table still show the narrow crystalline salt peaks, in addition to the prominent water ice peak at 3122 cm^{-1}, on the far left of the spectrum. The appearance of this ice peak is because the crystalline salt on top of the water ice in

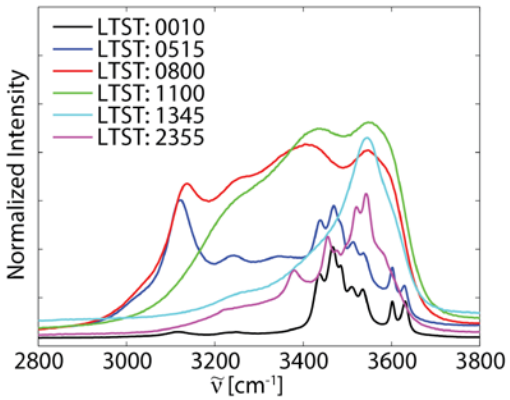

Figure 3. *Raman spectra in the O-H stretching band throughout the full diurnal cycle shown in Fig. 2. The shift to fewer but much broader peaks at 3578 cm^{-1} in the spectrum taken at 08:00 clearly indicates the presence of liquid solution.*

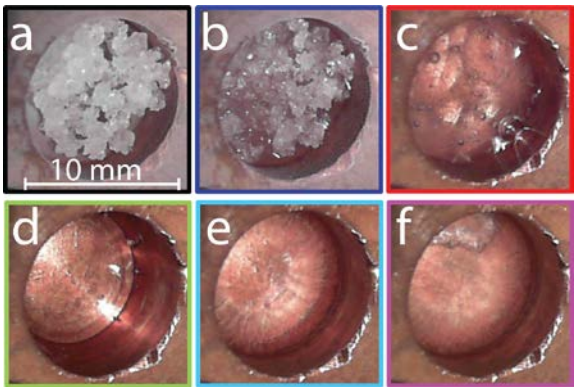

Figure 4. *Images of the sample, color-coded according to the spectra shown in Fig. 3. (a) Salt on top of ice at the start of the experiment at 00:10 when the temperature is below the eutectic value. (b) Evidence for brine at 05:15, shortly after the eutectic temperature is exceeded. (c) Salt has completely dissolved but water ice is still present at 08:00. (d) Only brine is present at 11:00. (e) Evidence for the presence of a salt crust at 13:45. The salt crust can be distinguished from the liquid by its different reflective properties. (f) Mainly crystalline salt hydrates with frozen brine below it at end of the diurnal cycle at 23:55.*

the sample has started to form brine and become more translucent for the Raman laser and the laser is picking up the signal from the water ice below. Nonetheless, the salt is still mostly solid and therefore the narrow crystalline salt peaks prevail between ~3400 and 3650 cm^{-1} and no liquid water peaks are detected. By 08:00 LTST Fig. 4c shows that the salt has completely dissolved into liquid brine on top of a remaining water ice layer. Also, the red line in Fig. 3 and the table show the prominent liquid water peak at 3578 cm^{-1}, instead of the narrower salt peaks. By 11:00 LTST the ice in the sample has completely melted and only brine remains (Fig. 4d) and, correspondingly, no ice peak appears in the decomposition. A salt crust starts forming at 13:45 LTST due to continuing evaporation of water from the sample (Fig. 4e) and after crossing the eutectic temperature again at ~23:00 LTST, the remaining brine freezes. This is indicated by the reappearance of the narrow perchlorate salt peaks in the O-H vibrational spectrum at 23:55 LTST and no remaining water peaks in the decomposition.

Discussion: Our results show that when water ice is in contact with $Ca(ClO_4)_2$ salt at Martian conditions, (liquid) brine can form within a few minutes of the eutectic temperature being exceeded in the layered case, and within ~45 minutes of the eutectic temperature being exceeded in the case of a mixed phase (frozen brine). As the temperature increases during the diurnal cycle, evaporation increases the concentration of the solution, causing a salt crust to form on the top of the sample, if the amount of ice available for the salt to melt is limited. The time of this depends on the

Reference Spectra						Sol 19 Diurnal Cycle of the Ground Temperature											
Salt		Ice		Water		LTST 0010		LTST 0515		LTST 0800		LTST 1100		LTST 1345		LTST 2355	
Peak	FWHM	Peak	FWHM	Peak	FWHM	Peak	FWHM	Peak	FWHM	Peak	FWHM	Peak	FWHM	Peak	FWHM	Peak	FWHM
		3046	99					3068	143								
		3115	57			3115	81	3122	60	3129	56						
		3227	206	3230	217	3249	113	3210	148	3219	280	3282	268	3256	219		
		3336	56													3311	271
		3399	140	3420	218	3437	147	3381	226	3434	224	3454	178	3495	249	3389	66
3446	37					3437	27	3440	31							3456	38
3471	20					3467	23	3470	24								
3487	24					3487	15	3488	16							3496	31
3515	29					3509	25	3512	28							3520	19
				3540	206					3578	114	3582	125	3555	106		
3542	25					3536	23	3539	23							3543	17
3564	70					3560	155	3569	122							3546	132
3603	17					3602	13	3602	15								
				3620	109												
3628	19					3630	18	3629	19								

Table 1: *Gaussian decomposition of the O-H stretching band of the reference Raman spectra of hydrated $Ca(ClO_4)_2$, water ice, and liquid water (left) [16], as well as of the Raman spectra shown in Fig. 3 (right). Each column contains the wavenumber and FWHM of each spectral peak. The values of the spectral peaks and their FWHM are color-coded to indicate the presence of salt (black), water ice (blue), common peaks of either water ice or liquid water (gray), and liquid water (red). The decomposition of the spectrum taken at 00:10, below the eutectic temperature, contains spectral peaks of hydrated perchlorate salt and water ice. In spite of the temperature being above the eutectic value and the image of the sample indicating that the ice starts to melt at 04:37, spectral peaks corresponding to liquid water are not observed at 05:15. The fact that the signal of the ice at the bottom of the sample is stronger at this time (the appearance of a shoulder caused by the 3068 cm^{-1} ice spectral peak and a general increase in intensity of all spectral peaks of ice, as shown in Fig. 3) provides indirect evidence that the ice has started to melt. The ice signal likely increases because the salt becomes more translucent when it absorbs liquid water, allowing the Raman laser to probe deeper layers in the sample. At 08:00 the Raman spectrum indicates the presence of liquid water unambiguously. The spectral peak at 3129 cm^{-1} indicates that water ice is still present, but by 11:00 this peak has disappeared. Evaporation of water causes the salt concentration of the solution to increase continuously until a salt crust forms at 13:45 (Fig. 4e). The decomposition still contains spectral peaks corresponding to brine because the signal from the thin crust is too weak for detection. Evaporation thickens the salt crust until crystalline salt dominates the spectrum at 23:55. Any possibly remaining brine freezes below the salt crust after the temperature drops below the eutectic value. The fit of each decomposition has an accuracy of ≥98%.*

amount of ice available. Due to the limited penetration depth of the Raman laser through the salt crust that developed on the sample, the exact time when a liquid phase ceased to exist in the sample could not be measured unambiguously. However, our results suggest that while the temperature was above the eutectic value for about 17 hours on sol 19 (Fig. 2), brine could have formed and persisted in the Dodo-Goldilocks trench as long as enough water ice was present to compensate for evaporation. Our analysis also indicates that brine forms at about 04:37 (i.e., minutes after the ground temperature exceeded the eutectic value), and freezes after about 22:20 (when the ground temperature decreased below the eutectic value). A possible kinetic delay between the temperature falling below the eutectic point and the freezing of the brine will be part of a future study.

Besides on exposed water ice layers like that uncovered by Phoenix, brine formation could also occur between polar and mid-latitudes regions, where frost and snow are seasonally deposited on saline soils [18, 19], water ice is seasonally present in the shallow subsurface [20] and temperatures exceed the eutectic value during a significant fraction of the sol [16; 21, 22]. Our results suggest that brine could form in the Martian polar region on seasonal time scales, persisting for as long as the temperature remains above the eutectic value during diurnal cycles because the melting of water ice could compensate for evaporation. Water ice is unlikely to be present in the shallow subsurface of mid-latitudes and equatorial regions because it is not thermodynamically stable in these places [2; 23]. However, frozen brine could be stable in the shallow subsurface of mid-latitude regions and brine could form temporally if the temperature exceeds the eutectic value. In addition, thin layers of frost are possible on polar facing slopes of those regions throughout the day [24], as well as on flat terrains at night [25]. Under these conditions, frost in contact with $Ca(ClO_4)_2$ salt could produce brine, but the persistence is limited by the short duration of the ground temperature being above the eutectic value and the frost having not completely sublimated away.

$Ca(ClO_4)_2$ salt was detected at the Mars Science Laboratory landing site at Gale Crater [7], where evidence for nighttime formation of frost a few tenths of

μm thick [26, 27] has been reported. However, frost can form at Gale only between 04:00 and 06:00 am, when the ground temperature is below the eutectic point. This thin layer of frost would have likely sublimated away by ~07:00, when the ground temperature first exceeds the eutectic value on the sols when frost is predicted [26]. In addition, the solubility of $Ca(ClO_4)_2$ salts in a film of water of a thickness of a few tenths of μm is unknown, indicating that brine is unlikely to form at the surface of Gale crater.

Bibliography: [1] Boynton, W. V., et al. (2002), Distribution of hydrogen in the near surface of Mars: Evidence for subsurface ice deposits, *Science 297*, 81-85. [2] Mitrofanov, I. et al. (2002), Maps of subsurface hydrogen from the High Energy Neutron Detector, Mars Odyssey, *Science 297*, 78-81. [3] Feldman, W. C. et al. (2002), Global distribution of neutrons from Mars Odyssey, *Science 297*, 75-78. [4] Smith, P. H. et al. (2009), H_2O at the Phoenix landing site, *Science 325*, 58-61. [5] Byrne, S. et al. (2009), Distribution of mid-latitude ground ice on Mars from new impact craters, *Science 325*, 1674-1676. [6] Hecht, M. et al. (2009), Detection of perchlorate and the soluble chemistry of Martian soil at the Phoenix Lander site, *Science 325*, 64-67. [7] Glavin, D. P. et al. (2013), Evidence for perchlorates and the origin of chlorinated hydrocarbons detected by SAM at the Rocknest aeolian deposit in Gale Crater, *J. Geophys. Res. 118*(10), 1955-1973. [8] Ming, D. W. et al. (2014), Volatile and organic compositions of sedimentary rocks in Yellowknife Bay, Gale crater, Mars, *Science 343*(6169), 1245267. [9] Renno, N. O. et al. (2009), Possible physical and thermodynamical evidence for liquid water at the Phoenix landing site, *J. Geophys. Res. 114*, E00E03. [10] Cull, S. C. et al. (2010), Concentrated perchlorate at the Mars Phoenix landing site: Evidence for thin film liquid water on Mars, *Geophys. Res. Lett. 37*(22). [11] McEwen, A. et al. (2011), Seasonal flows on warm Martian slopes, *Science 333*, 740-743. [12] Martín-Torres, F. J. et al. (2015), Transient liquid water and water activity at Gale crater on Mars, *Nat. Geosci. 8*, 357-361. [13] Ojha, L. et al. (2015), Spectral evidence for hydrated salts in recurring slope lineae on Mars, *Nat. Geosci. 8*(11), 829-832. [14] Kounaves S. P. et al. (2014), Identification of the perchlorate parent salts at the Phoenix Mars landing site and possible implications, *Icarus 232*, 226-231. [15] Marion, G. M. et al. (2010), Modeling aqueous perchlorate chemistries with applications to Mars, *Icarus 207*(2), 675-685. [16] Fischer, E. et al. (2014), Experimental evidence for the formation of liquid saline water on Mars, *Geophys. Res. Lett. 41*, 4456-4462. [17] Savijärvi, H. I. and Määttänen, A. (2010), Boundary-layer simulations for the Mars Phoenix lander site, *Q. J. R. Meteorol. Soc. 136*(651), 1497-1505. [18] Whiteway, J. A. et al. (2009), Mars water-ice clouds and precipitation, *Science 325*, 68-70. [19] Martínez, G. M. et al. (2012), The evolution of the albedo of dark spots observed on Mars polar region, *Icarus 221*, 816-830. [20] Cull, S. C. et al. (2010), Seasonal ice cycle at the Mars Phoenix landing site: 2. Postlanding CRISM and ground observations, *J. Geophys. Res.: Planets 115*, E00E19. [21] Möhlmann, D. T. F. (2011), Latitudinal distribution of temporary liquid cryobrines on Mars, *Icarus 214*(10), 236-239. [22] Nuding D. L. et al. (2014), Deliquescence and efflorescence of calcium perchlorate: An investigation of stable aqueous solutions relevant to Mars, *Icarus 243*, 420-428. [23] Schorghofer, N. and Aharonson, O. (2015), Stability and exchange of subsurface ice on Mars, *J. Geophys. Res.: Planets 110*, E05003. [24] Vincendon, M. et al. (2010), Water ice at low to midlatitudes on Mars, *J. Geophys. Res. 115*(E10). [25] Wall, S.D. (1981), Analysis of condensates formed at the Viking 2 lander site: The first winter, *Icarus 47*(2), 173-183. [26] Martínez, G. M. et al. (2015), Likely frost events at Gale crater: Analysis from MSL/REMS measurements, *Icarus 280*, 93-102. [27] Savijärvi, H. I. et al. (2015), Mars Science Laboratory diurnal moisture observations and column simulations, *J. Geophys. Res.: Planets 120*, 1011-1021.